ANL-76-6

# PHYSICS OF REACTOR SAFETY

## Quarterly Report
## July—September 1975

ARGONNE NATIONAL LABORATORY, ARGONNE, ILLINOIS
Prepared for the U. S. NUCLEAR REGULATORY COMMISSION
Office of Nuclear Regulatory Research

Printed in the United States of America
Available from
National Technical Information Service
U. S. Department of Commerce
5285 Port Royal Road
Springfield, Virginia 22161
Price: Printed Copy $5.00; Microfiche $2.25

Distribution Category:
Advanced Reactor Safety
Research—Fast Reactors
(NRC-7)

ANL-76-6

ARGONNE NATIONAL LABORATORY
9700 South Cass Avenue
Argonne, Illinois 60439

# PHYSICS OF REACTOR SAFETY

Quarterly Report
July—September 1975

Applied Physics Division

Work performed for the
Division of Reactor Safety Research
U. S. Nuclear Regulatory Commission

Previous reports in this series:

ANL-75-31 January—March 1975
ANL-75-67 April—June 1975

TABLE OF CONTENTS

## LIST OF FIGURES



## LIST OF TABLES

# PHYSICS OF REACTOR SAFETY

Quarterly Report
July—September 1975

## I. ABSTRACT

This quarterly progress report summarizes work done in Argonne National Laboratory's Applied Physics Division for the Division of Reactor Safety Research of the U. S. Nuclear Regulatory Commission during the months of July-September 1975. It includes reports on reactor safety research and technical coordination of the RSR safety analysis program by members of the Reactor Safety Appraisals Group, Monte Carlo analysis of safety-related critical assembly experiments by members of the Theoretical Fast Reactor Physics Group, and planning of DEMO safety-related critical experiments by members of the Zero Power Reactor (ZPR) Planning and Experiments Group.

## TECHNICAL COORDINATION - FAST REACTOR SAFETY ANALYSIS (A2015)

## II. SUMMARY

Further studies were carried out on sodium voiding rates in the 4000 MWe LMFBR model with the old and new PRIMAR model. For flow decay periods of 10-11 seconds average ramp rates with both PRIMAR versions gave average ramp rates of \$20-30/second. For decay periods of 6-7 sec the new PRIMAR gave about the same results as with slower flow decay, while average ramp rates with the old PRIMAR were ∿\$40/sec. There was not much effect of Doppler coefficient on ramp rate over a considerable range of variation.

FX2-POOLVENS has been used to study the importance of fuel/steel heat transfer in HCDA's. It was concluded that such heat-transfer effects are not important in an initial disassembly, but are important in the study of boiling pools which might form subsequently.

Programming has continued on the improved fuel/coolant interaction (FCI) model. Almost all the final options have now been built into the code, which is almost ready to be compiled so that debugging and testing can start.

A corrected method has been developed for calculating axial expansion effects in SAS. The new method gives results 33 to 43% of those obtained from the formula in the present SAS code.

The rate of heat transfer between a hot gas or vapor and a colder one on sudden mixing, which might be of interest in FCI calculations, has been studied. The time constant for heat transfer has been found to be of the order of $10^{-8}$ seconds, indicating that instantaneous thermal equilibrium on mixing may be assumed.

The WARD code DEMO was received through the Argonne Code Center and has been implemented on the IBM 370. Considerable difficulties were experienced in the conversion, mainly occasioned by undefined variables (a problem for IBM FORTRAN but not for CDC) and by a number of errors in the code. The appropriate corrections have been made and transmitted to the Code Center and to WARD. The code appears to be executing successfully now.

Meetings were held with staff members of the Sandia Laboratory to discuss preparation of elements of the RSR Program Plan and also to discuss the RSR program at Sandia and how ANL might cooperate in it. Meetings were held at LASL with staff members there to discuss progress in the SIMMER code development and how ANL could assist in this effort. There was also a discussion of comparative HCDA disassembly calculations at LASL.

Drafts of a number of elements of the RSR Program Plan were completed and forwarded to RSR.

## III. STUDY OF BASIC PROBLEMS IN ACCIDENT ANALYSIS

### A. Initiating Condition Variations

#### 1. Pump Coastdown Calculation for a Model of a 4000 MWe Oxide-Fueled LMFBR (H. Hummel, P. Pizzica)

Further studies were carried out on voiding rates in the 4000 MWe LMFBR model[1,2] to try to better quantify differences between use of the old and new PRIMAR. Doppler coefficient and flow coastdown rate were used as parameters in these studies. Results are given in Table I. In this Table the "original" Doppler coefficients are the ones we calculated for this model. The reduced ones are less than the original ones by 10% for sodium in and by 20% for sodium voided, which is about what Bleiweis et al[2] used in their calculations. The "reduced-20%" values are reduced another 20% beyond this. The motivation in reducing the Doppler coefficient is to see if autocatalytic tendencies develop in sodium voiding. The results show no consistent trend of sodium voiding ramp rate with Doppler coefficient in the range studied.

Fuel slumping was suppressed up to a maximum fuel temperature of 4500°C and the calculation was terminated at this point because fuel-melt fractions were about 90%, and it was felt that the calculation would not be physically meaningful at higher fuel energies. There was some tendency for ramp rate to increase with fuel energy, but maximum values were still far below the $250/sec observed by Bleiweis et al.

The approximate flow decay period is defined as the exponential period that would produce the observed fractional flow decay. Because the decay was not really exponential this number has somewhat limited significance. In Table I values of this period are given based on the fractional flow decay obtained at 9.0 sec after start of the flow reduction and also at 12.0 sec. Actual fractional flow decays obtained at various times using the indicated pump head decay coefficients are also given in Table I. These fractional decays are given until the time boiling started.

Table I. Summary of Results for Sodium Voiding Ramp Rates Using PRIMAR I and II for 4000 MWe Oxide-Fueled LMFBR

| PRIMAR | Approx. Flow Decay Period, Sec. Based on Decay at 9.0 sec / 12.0 sec | | PDEC[a] | PDEC1[a] | PDEC2[a] | Doppler Coefficients | Range of Ramp Rates, $ /sec | Average Ramp Rate, $/sec | Fractional Flow Decay @ 3.0 sec | 6.0 sec | 9.0 sec | 12.0 sec | 15.0 sec |
|---|---|---|---|---|---|---|---|---|---|---|---|---|---|
| II | 6.5 | | 0.380 | $-6.43\times10^{-3}$ | $8.23\times10^{-4}$ | Original | 10-36 | 22 | 0.656 | 0.406 | 0.250 | --- | --- |
| | | | | | | Reduced-20% | 12-29 | 18 | | | | | |
| II | 8.3 | | 0.280 | $-6.43\times10^{-3}$ | $8.23\times10^{-4}$ | Original | 14-25 | 20 | 0.721 | 0.507 | 0.338 | --- | --- |
| | | | | | | Reduced | 14-23 | 21 | | | | | |
| | | | | | | Reduced-20% | 18-26 | 20 | | | | | |
| II | 8.9 | 10.2 | 0.3108 | $-1.6563\times10^{-2}$ | $3.426\times10^{-4}$ | Original | 9-24 | 13 | 0.650 | 0.466 | 0.364 | 0.304 | --- |
| II | 11.0 | 10.1 | 0.200 | $-6.43\times10^{-3}$ | $8.23\times10^{-4}$ | Original | 13-31 | 21 | 0.795 | 0.605 | 0.442 | 0.303 | --- |
| | | | | | | Reduced | 16-26 | 19 | | | | | |
| | | | | | | Reduced-20% | 16-25 | 15 | | | | | |
| I | 6.4 | | 0.240 | $-6.43\times10^{-3}$ | $8.23\times10^{-4}$ | Original | 27-57 | 40 | 0.683 | 0.449 | 0.247 | --- | --- |
| | | | | | | Reduced | 31-62 | 39 | | | | | |
| | | | | | | Reduced-20% | 26-50 | 41 | | | | | |
| I | 6.9 | | 0.35393 | $-1.6563\times10^{-2}$ | $3.426\times10^{-4}$ | Reduced-20% | 21-53 | 32 | 0.596 | 0.390 | 0.273 | --- | --- |
| I | 10.8 | 8.2 | | | | Original | 28-60 | 42 | 0.783 | 0.621 | 0.436 | 0.230 | --- |
| | | | | | | Reduced-20% | 27-52 | 38 | | | | | |
| I[b] | 8.1 | 9.3 | 0.35393 | $-1.6563\times10^{-2}$ | $3.426\times10^{-4}$ | Original | 17-29 | 22 | 0.618 | 0.432 | 0.333 | 0.276 | 0.239 |
| I | 8.9 | 10.2 | | | | Original | 18-32 | 24 | 0.650 | 0.466 | 0.364 | 0.304 | --- |
| | | | | | | Reduced | 24-41 | 31 | | | | | |
| | | | | | | Reduced-20% | 19-42 | 31 | | | | | |

[a] Coefficients in pump head decay equation $\Delta P/\Delta P_o = \exp\left[-PDEC*t - PDEC1*t^2 - PDEC2*t^3\right]$

[b] SAS 2A was used in this calculation. All others used SAS 3A.

There does not seem to be any consistent dependence of sodium voiding ramp rate on flow decay rate for PRIMAR-II. For PRIMAR-I there seems to be a trend toward higher ramp rates at higher flow decay rates. Although there does not seem to be much difference between voiding ramp rates with PRIMAR-I and PRIMAR-II at lower flow decay rates, at more rapid flow decay these ramp rates are consistently larger for PRIMAR-I, as had been expected. The one case run with SAS-2A, which had a voiding model believed to be same as that used by Bleiweis et al, gave results comparable to and even slightly lower than those obtained with SAS-3A at a similar flow coastdown rate.

## B. Model Studies

### 1. Studies of the Importance of Fuel-Steel Heat Transfer in HCDA's Using FX2-POOLVENS (P. Abramson)

A modification to POOLVENS--the version of POOL which is linked to FX2--was completed which resulted in a reduction of POOL subroutine computing time of roughly 50% and a decrease in its core storage requirements by 90K. This resulted in a savings of about 7% of overall FX2-POOL running time and a reduction of (full program) core storage to 1280K.

FX2-POOLVENS was used to examine the importance of fuel/steel heat transfer in HCDA's. Two very different HCDA's were examined.

Case 1 corresponds to a rapid disassembly in a 1000 MWe reactor (as studied by Bleiweis et al.[3]) which begins its study at 100 times nominal power and \$50/sec ramp starting from \$1.05. In this particular study the heat transfer rate has varied by 3 orders of magnitude and the corresponding change in energy deposited was roughly 10%.

Case 2 corresponds to the original benchmark slow disassembly study used for comparison of FX2-POOL, VENUS II[4] and PAD.[5] It is a CRBR-like reactor beginning from $10^9$ watts at \$1.05 and around \$100/sec (the case studied for benchmark used \$50/sec). In this portion of the study, heat transfer rate was varied by 3 orders of magnitude and initial steel temperature set at 800°K. Several interesting results are observed below.

In both Case 1 and 2, the ramps were generated, as one must with FX2, by material motions. These material motion rates were set at a constant value for each case and only the heat transfer rates were varied. We observe in Case 2 that varying the heat transfer coefficients caused the ramp rate to vary from a minimum of about \$100/sec to a maximum of \$700/sec. We further observe that in Case 2, the case with the highest ramp rate (which has the highest energy deposition) is the case with the highest heat transfer rates, and the ramp was caused (see Fig. 3) by a positive Doppler feedback caused by fuel cooling.

In POOLVENS, the heat transfer from fuel to steel was characterized by an expression of the form

$$\frac{\Delta E}{\Delta t} = C_1 A_1 (T_{fuel} - T_{steel}) \ (\alpha) + \sigma\varepsilon (T_{fuel} - T_{steel}) A_1$$

$\sigma$ is the Stefan constant,
$\varepsilon$ is the grey to grey emmissivity ($\sim$0.54),
$\alpha$ is the relative fuel volume fraction (since heat is transferred only from the fuel) and
$C_1$ and $A_1$ are the parameters varied
$C_1$ represents a convective heat transfer coefficient from fuel to steel
$A_1$ represents the steel droplet area, and also enters into determining the steel temperature through the surface to volume ratio for steel.

In Fig. 1, we show power vs time for Case 1. Since Case 2 is slower, there is more time for heat transfer to be important and we show several families of curves for Case 2 (See Table II).

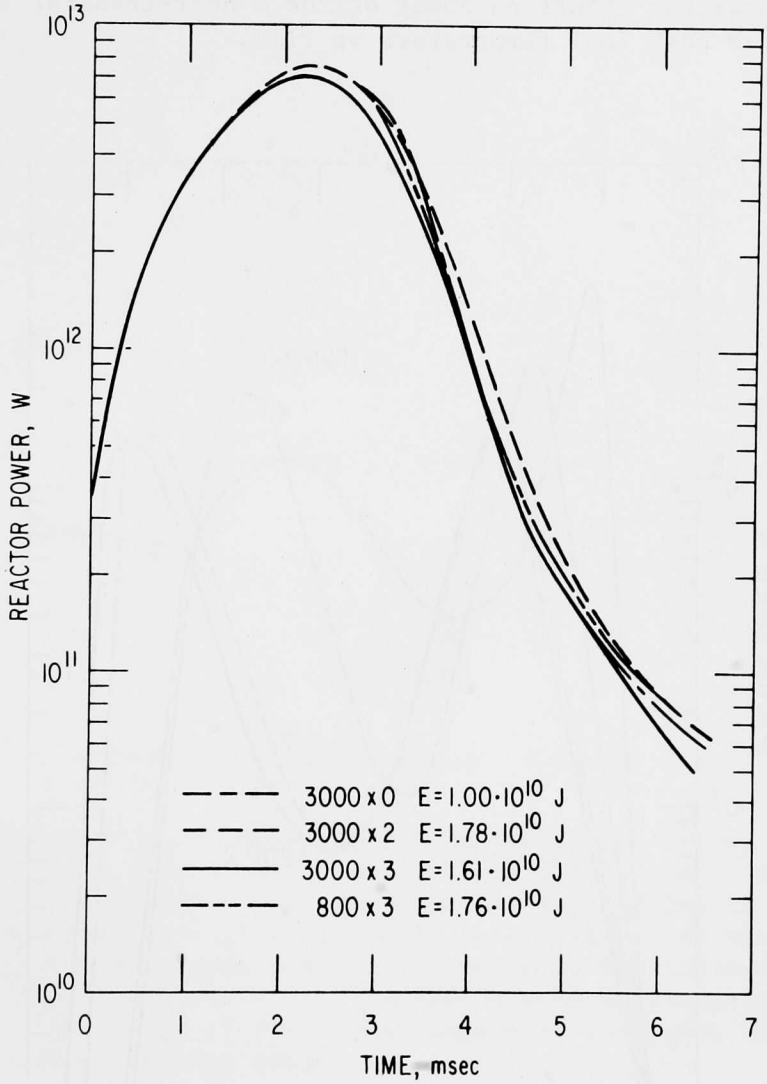


Fig. 1. Reactor Power vs. Time For Case 1

TABLE II. Study Parameters and Results for Case 2

| Run No. | $C_1$ | $A_1$ | Peak $T_{fuel}$ | E deposited | Initial ramp |
|---|---|---|---|---|---|
| 1 | 1.0 | 1.0 | 5734°K | $5.63 \cdot 10^9$J | \$99/sec |
| 2 | 1.0 | 0.1 | 5684°K | $5.69 \cdot 10^9$J | \$100/sec |
| 3 | 1.0 | 0.01 | 5369°K | $6.02 \cdot 10^9$J | \$105/sec |
| 4 | 100.0 | 1.0 | 5373°K | $7.66 \cdot 10^9$J | \$164/sec |
| 5 | 100.0 | 0.01 | 4450°K | $10.37 \cdot 10^9$J | \$687/sec |

(Higher $C_1$ and lower $A_1$ give more rapid heat transfer)

Figure 2 shows the effect on power of the 5 heat-transfer combinations, and Figure 3 shows peak fuel temperature vs time.

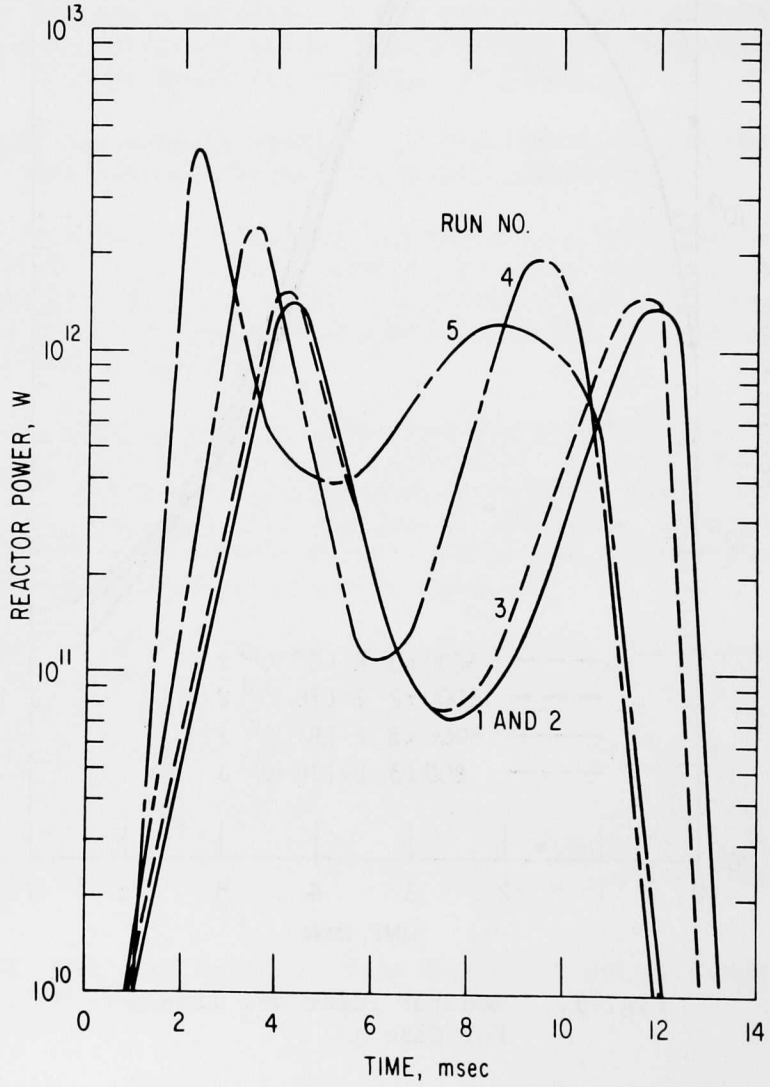


Fig. 2. Reactor Power vs. Time for Case 2

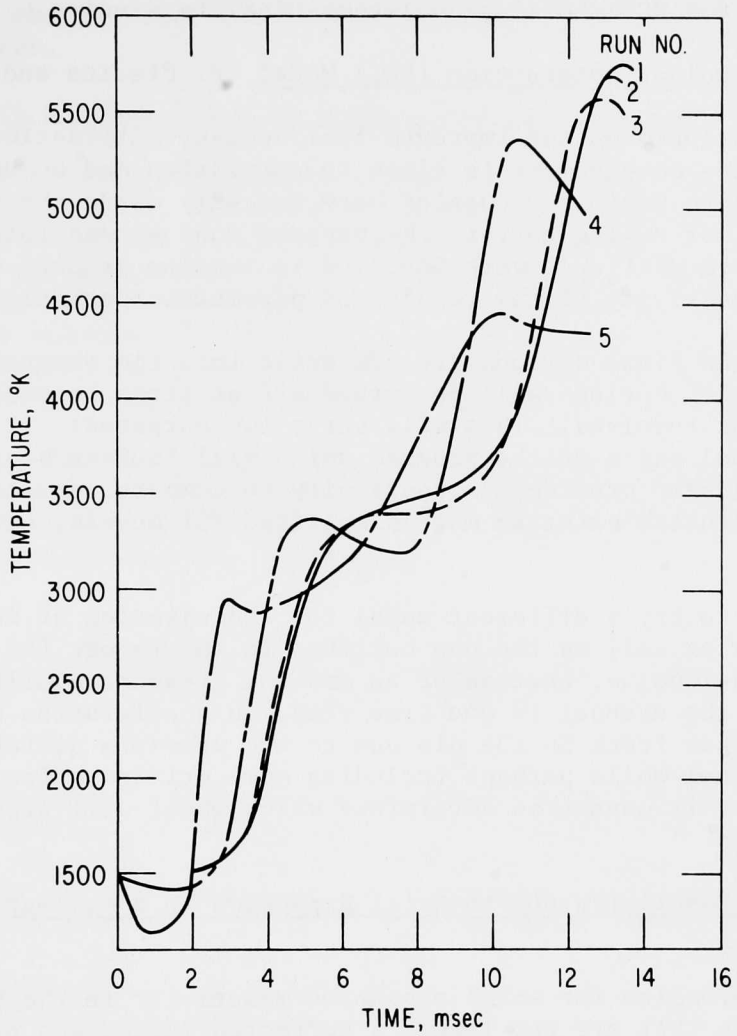


Fig. 3. Peak Fuel Temperature vs. Time for Case 2

It is interesting to observe the strong influence of heat transfer in retarding the Doppler effect (previously observed by Jackson and Nicholson[4] in a study of the influence of FCI on HCDA's). This effect is probably not important in the study of HCDA's, since it is unlikely that mixing good enough to carry us much beyond Case 3 will occur in the initial CDA stages. However, this effect can play a very important role in analyzing the boiling pool situation and will be of particular impact in analyzing the "Fauske picture" of fluidized boiling pools.

We conclude:

1. There seems to be no need to concern ourselves with the heat transfer effects in examining neutronic energy deposition in initiation CDA's (however, these effects could be important in examining the work potential).

2. The results of the calculations seem physically reasonable and serve further to provide confidence in the use of the FX2-POOL technique for HCDA/boiling-pool-recriticality studies.

2. Improved Fuel-Coolant Interaction (FCI) Model (P. Pizzica and P. Abramson)

Programming continued on the improved fuel/coolant interaction model. This phase of the code development is close to completion and debugging of the program is about to begin. Debugging here not only means the relatively straightforward task of making certain the program runs as was intended but also includes the more difficult work involved in testing aspects of the model and checking the sensitivity of the results to parametric variations.

Almost all of the final options are now built into the program but, in order to test the code, options will be turned off at first in order to simplify the calculations involved. This will serve two purposes: it will allow checking of individual parts of the program which will isolate sources of problems and it will also provide an opportunity to compare results (as far as this can be done) with the existing more simplified FCI models, especially PLUTO.

It was decided to try a different model for the ejection of fuel from the pin into the channel as well as the one outlined in the report for the previous quarter. This would involve, instead of an assumed pressure equilibration between the pin and the channel in one time step, an acceleration of the molten fuel/fission gas froth in the pin due to the pressure difference between the pin and the channel while perhaps including some orifice effects. Until some testing is done, it cannot be determined which model will produce better results.

3. Calculation of Reactivity Due to Axial Expansion in a Nuclear Reactor (Kalimullah)

Because the expression for axial expansion reactivity in the SAS code was known to give results that are too large, a corrected method was developed. The case of a finite-cylindrical bare homogeneous one-group reactor was examined first. For this simple case, analytical expressions were derived for the axial expansion reactivity first by an exact method and then by using a reactivity distribution obtained by the first-order perturbation theory. These expressions are found to be identical. Since most computer programs for transient analysis of fast reactors, e.g., the SAS code, use reactivity tables pre-calculated by perturbation theory, the method used for calculating the axial expansion reactivity using a reactivity distribution formula for the above simple case has been extended to the reactor geometry model used in the SAS code. The study of the simple case provides an insight into the validity of the present method, but not a general proof. A Fortran program has been written to calculate the axial-expansion reactivity using the present method. This program may be called by the SAS code to obtain the reactivity due to axial expansion by channel. For the 6 subassemblies of row 2 of CRBR at BOFC, the reactivities due to axial expansion of fuel computed by the present method turns out to be 33 to 43% of those obtained by the formula in the present SAS code.

The axial expansion of the reactor discussed here may or may not be caused by temperature changes. If an axial expansion has been caused by a temperature change, then the reactivity calculated here does not include the Doppler effect.

4. A Theory of Heat Transfer Between Two Gases in a Mixture (Kalimullah)

In the analysis of hypothetical core disruptive accidents of liquid metal fast breeder reactors, one needs to evaluate the rate of heat transfer between a hot gas or vapor and a colder one which are already mixed together by the macroscopic agitation existing in the system, for example, the heat transfer between sodium vapor and fission gases or that between sodium vapor and $UO_2$ vapor in the analysis of a fuel-coolant interaction following a clad rupture. This analysis may be important not because of the amount of energy involved in this transfer but for calculating the pressure of such a mixture of gases.

Starting from the mechanics of collision between two perfectly elastic smooth spherical molecules, the following equation for the heat transfer rate per unit volume from a gas or vapor 2 to another gas 1 in a mixture is derived based on the kinetic theory of gases:

$$\left.\frac{dE}{dt}\right|_{2\to 1} = \frac{8k\sqrt{2\pi k}\, a^2 \rho_1 \rho_2}{(m_1 + m_2)^2} \left(\frac{T_1}{m_1} + \frac{T_2}{m_2}\right)^{\frac{1}{2}} (T_2 - T_1),$$

where a is the sum of their molecular radii, $m_i (i=1,2)$ are masses of the molecules, $\rho_i$ are densities of the gases, $T_i$ their absolute temperatures and k is Boltzmann's constant. Methods of estimating molecular diameters when experimental values are not available, are indicated and values for sodium and $UO_2$ vapor are estimated. For a set of typical values of the parameters, the time constant for the heat transfer is found to be of the order of $10^{-8}$ sec which implies that for processes occurring in time periods greater than those of the order of $10^{-8}$ sec, the gases may be assumed to come to a thermal equilibrium at the instant they mix.

C. Programming Development

1. Implementation of the DEMO Code on the IBM 370 195 (Kalimullah)

In order to be able to study external plant effects on accident sequences, (e.g., the possibility of decay heat removal by natural circulation in the primary loop in the event of a large or small pipe rupture or of a power failure with scram), a copy of the DEMO code was obtained from WARD in the CDC Display Code. After translating into EBCDIC, the following modifications and corrections were made in the source:

The variables NDRUM, OMDEL, TIME, HFW, KCP, TCHK, QTTS, POINT(11), TOUT(1), DTPLOT, and arrays P(50), DTNODE(50), KCRIT(30), VOIDF(50), DTCONN(30), and ZP(4) were left undefined originally. In consultation with WARD, these variables have been defined. A number of subroutine, common block and variable names are changed as shown in Table III, because of the differences between the FORTRAN used by CDC and IBM machines. A new BLOCK DATA subprogram was

TABLE III. Name Changes in the DEMO Code

| VARIABLES | | COMMON LABELS | | SUBROUTINES | |
|---|---|---|---|---|---|
| Old Name | New Name | Old Name | New Name | Old Name | New Name |
| PROTDUM | AIBM2 | PROTOUT | AIBM1 | USERMAN | MAIN |
| SODMASS | AIBM3 | HOTCHAN | AIBM10 | CONTROL | AIBM12 |
| DPNATPI | AIBM4 | DFLOPRI | AIBM11 | REACTOR | AIBM13 |
| DPNATIR | AIBM5 | STEAM | AIBMA | RUPTURE | AIBM14 |
| DPNATXI | AIBM6 | New | AIBMB | PROTSYS | AIBM15 |
| DPNATIS | AIBM7 | New | PLTPT | POLATE1 | AIBM18 |
| DPNATSE | AIBM8 | TIME | BIBM | POLATE2 | AIBM19 |
| DPNATEI | AIBM9 | IOPRT | BBIBM | RODFAIL | AIBM21 |
| PNERTIA | AIBM16 | SUSPLT | BBBIBM | SUPXACT | AIBM22 |
| SNERTIA | AIBM17 | | | FRICFAC | AIBM24 |
| FLUXTAU | AIBM20 | | | New | BLOCK DATA |
| SUSPLOT | AIBM23 | | | New | TLFL |
| | | | | New | SECOND |

written to initialize those variables which were originally initialized by DATA statements in subroutines USERMAN(=MAIN), CAVP, RUPTURE(=AIBM14), IODATA and STMGEN, and belonged to common blocks. As shown in Table III, some new common blocks and subroutines were also put in. Correction of some errors in the subroutine STMGEN received from WARD has also been incorporated. The variable NS has been declared real in three more subroutines. In the original code some DO loop indices and subscripts became zero. Circumventions for these have been put in the new source. A number of modifications have been made and new variables (AIBM27, AIBM28, . . . , IIBM1, IIBM2, . . .) introduced in changing the form of some DATA statements in various subroutines, and in supplying missing arguments in some CALL statements. The Code has been modified to point the final tabular output after only 10 (instead of 40) fine points have been accumulated so that a large amount of computer time is not lost if the job fails.

The following variables are printed by the Code but were left undefined in the program. These were not defined as a part of the corrections made because they were found not to have been used in any calculation during execution.

(1) DXTP2(1) one card above statement No. 40 in MAIN

(2) PNATI(3) one card below statement No. 2015 in MAIN

(3) PS(3) one card below statement No. 2022 in MAIN

(4) TORQ(6) and HD(6) one card below statement No. 2017 in MAIN

(5) IDATE in common block BIBM (previously named TIME) printed in subroutine SUSOD.

Copies of the list of the above corrections and modifications, and the listing of the new source have been sent to WARD and the Argonne Code Center.

With the above changes, the code has been run on our IBM machine up to a transient time of about 1.26 sec for the sample problem obtained from WARD. After 1.26 sec the time step per cycle becomes practically zero perhaps due

to the instability caused by roundoff in the single precision arithmetic. In the case of an instability, the Code reduces the timestep, thinking that it is too large. At the transient time of about 1 sec the answers seem to agree with those in a run made at WARD. A double precision version of the new Code has been prepared and appears to be executing satisfactorily in first tests.

## IV. COORDINATION OF RSR SAFETY ANALYSIS RESEARCH

### A. Program at Sandia Laboratory

An introductory meeting was held to discuss program plan elements and to survey the Sandia RSR programs by P. Abramson on July 2, 1975. Discussions were held primarily with R. Coats and his staff.

On September 15, 1975 H. Hummel and P. Abramson visited Sandia for coordination initiation meetings with R. Coats, D. Dahlgren, R. Jefferson and B. Butcher. Discussions were held regarding their Equation-of-State efforts, their fuel/steel melting experiments and some brief discussions of the role ANL might play in assisting their hydro/thermodynamic studies.

### B. Program at Los Alamos Scientific Laboratory

Abramson and Hummel together with R. Curtis of RSR were at LASL on September 18 to discuss the SIMMER program with LASL personnel, including M. Stevenson, J. Boudreau, L. Smith, and P. Bleiweis. The URANUS code is being used to test various features of SIMMER. The question of whether or not to incorporate a quasistatic option in SIMMER is being studied. The hydrodynamics in the initial release, SIMMER-I, expected by the end of 1975, will be the 2-field 3-component KACHINA. Implementation of the improved modeling in SHALAKO has been deferred. Work is still proceeding on the psuedo-field in SIMMER that will represent can walls, wire wrap, and solid fuel. For the psuedo field account will be kept of energy and mass at every node, with a simple modeling of heat transfer. The psuedo-field will be assumed infinitely strong until failure. Melting of structure and freezing and plugging of droplets on cold structure will be modelled in some simple fashion.

The initial release of SIMMER will use microscopic Bondarenko cross sections although the computing time with that procedure appears rather lengthly. A long running time for the whole code seems indicated on the basis of present information.

The method of obtaining initial conditions for SIMMER is still undecided. For the present, output from SAS calculations for the CRBR and 1000 MWe models will be used to estimate reasonable starting conditions. The need to model undamaged core in some way is recognized, but it is felt that the use of the detail in SAS is not feasible. At present use of a lumped parameter model in which an axial segment of a fuel pin is represented by a single node is being studied.

Ways in which Abramson could cooperate in the SIMMER work were discussed. Although SIMMER-I is to be implemented on both CDC-1600 and IBM machines, it was not immediately clear that it will be feasible for us to use it because of the long running time and local conversion problems. Possible use of the

URANUS code at ANL was discussed, but did not seem feasible. The most promising immediate step appears to be to put KACHINA in FX-2 POOL. Abramson felt this would not be difficult, and Boudreau will forward a deck and manual for KACHINA to Abramson. Boudreau suggested that Abramson could also be helpful in estimating values of coefficients needed in SIMMER such as liquid-vapor drag coefficients, heat transfer parameters, and distribution droplet sizes, etc.

An important application of SIMMER is in studying the validity of H. Fauske's hypothesis that following a disassembly the core material remains boiled up and therefore subcritical for a sufficient time that any plugs of frozen material above and below the core that prevent permanent dispersal of the core would be melted away before recriticality would be possible. LASL has started to study this problem for a single subassembly region. It seems desirable to study it for a region constituting a major fraction of the core as soon as possible. This problem cannot be handled accurately with FX2-POOL at present because the importance of vapor-liquid slip is not known and can only be crudely investigated with POOL. It may be that the use of KACHINA in place of POOL's hydrodynamics routines will make such a study possible, however.

Abramson also conferred with J. F. Jackson at Brigham Young University concerning disassembly calculations. Jackson indicated his belief that VENUS-II does not take account of the heat of vaporization in disassembly, a point on which there has been some confusion.

Abramson also conferred with T. McLaughlin concerning comparison calculations for the disassembly phase of an HCDA. Vapor generation energy calculation seem to be consistent between PAD and FX-2 POOL.

C. Miscellaneous

Abramson presented a seminar on the FX2-POOL program at Germantown on July 16 for NRC and ERDA personnel.

Abramson and Hummel attended a meeting on the transient overpower accident for LMFBR's conducted by DRL in Bethesda September 24 and 25.

Drafts of the following elements of the RSR Program Plan were completed and transmitted to RSR:

1.3.4 Transition Phase Kinetics

1.8.2 Initial Core Material Motions

1.8.4 Post Diassembly Considerations

(P. Abramson)

1.8.1 Voiding Dynamics and Doppler Effects

2.1.1 Accident Initiation Models

2.1.2 Accident Progression and Systems Interaction

2.2.6 Models of Reactivity Feedback

3.1.1 Propagation of Local Failures

3.1.2 Transient Overpower Tests

3.1.3 Transient Undercooling Tests

3.1.9 Reactivity Effects

(H. Hummel)

## MONTE CARLO ANALYSIS AND CRITICALS PROGRAM PLANNING FOR SAFETY-RELATED CRITICALS (A2018)

## V. MONTE CARLO ANALYSIS OF SAFETY RELATED CRITICALS

### A. Status of Work on ZPR-3 Assembly 27 (E. Gelbard)

The VIM analyses of ZPR-3 Assemblies 27 and 28 have now been completed. VIM eigenvalues for Assembly 27 are tabulated below:

| | | |
|---|---|---|
| ENDF/B-III | 1.001 ± 0.003 | (100 generations, 1000 histories per generation) |
| ENDF/B-IV | 1.005 ± 0.003 | (100 generations, 1000 histories per generation) |
| ENDF/B-III ($^{235}$U density raised by 1.5%) | 1.007 ± 0.003 | (100 generations, 1000 histories per generation) |

The confidence intervals indicated here are standard deviations. It should be noted however, that there is a substantial uncertainty concerning the loading of this assembly. Thus, for example, the net $^{235}$U loading reported by the experimentalists is 1.5% higher than the loading computed directly from the drawer masters. The first two eigenvalues listed above were computed with $^{235}$U densities taken from hot constants tables for each individual fuel plate in each drawer master. In order to estimate the effect of uncertainties in the loading, the number densities of $^{235}$U in each plate were then raised by 1.5% and the eigenvalue was recalculated. It will be seen that a 1.5% uncertainty in the net $^{235}$U inventory corresponds, in this case, to more than a 0.5% uncertainty in k.

The 100-generation calculations described above were started from fairly crude fission source guesses. Since Assembly 27 is very leaky, the outer iterative process should converge very quickly, so that errors in the source guess should have little effect on the accuracy of eigenvalue estimates averaged over 100 generations. In fact the eigenvalue estimates change very little if the first hundred generations are discarded. Eigenvalue estimates based on the last 80,000 histories are listed below.

| | |
|---|---|
| ENDF/B-III | 1.000 ± 0.003 |
| ENDF/B-IV | 1.006 ± 0.003 |
| ENDF/B-III ($^{235}U$ density raised by 1.5%) | 1.006 ± 0.003 |

It will be seen that there is no indication of a significant bias in the discarded 20 generations.

VIM calculations for Assembly 28 were carried out only with ENDF/B-III cross sections. For Assembly 28, after 100,000 histories, we get $\lambda$ = 0.992 0.003, and discarding the first 20 generations (i.e., the first 20,000 histories), $\lambda$ = 0.994 ± 0.003. The inventory uncertainty is, however, even greater for Assembly 28 than for Assembly 27. In the case of Assembly 28 the net $^{235}U$ inventory reported by the experimentalists is 3% greater than the $^{235}U$ loading deduced from loading diagrams.

It seems clear from the above results that the VIM eigenvalues for Assemblies 27 and 28 agree with experiment to within about one percent. In view of the uncertainties in loading, little more can be said about these particular assemblies. The calculations do demonstrate, however, that it is possible to input extremely complicated plate lattice configurations into VIM, plate by plate, in full detail.

## VI. PLANNING OF DEMO SAFETY RELATED EXPERIMENTS

Several different facets of the planning activity are included in this quarterly report. As a result of this planning work a brief statement of the justification for meltdown safety-related critical experiments has been prepared. It is included. The relationship of other critical experiment programs to this planning activity is examined in some detail. The result of this examination has lead to some modifications of the scope and objectives of the program currently being planned. The key characteristics of the core design for the criticals program are discussed, and the results of the initial core-design calculations are tabulated and discussed.

### A. Justification for Safety-Related Critical Experiments Program

A large number of fast-reactor critical experiments have been performed over the past several years to check and to validate the data and codes used in fast-reactor analysis. In spite of this effort there are still several areas where there are significant discrepancies between the analysis and experiments. For example, eigenvalues around 0.98 or 0.99 are normally calculated for these systems, some key reaction-rate ratios disagree a few percent with

calculations, and the central-worth discrepancy remains. It is only within the past few years that enough data have become available to enable careful studies of fast-reactor calculations, and improvements in the calculations are now being observed. This, of course, reflects the code developments and data adjustments that have been made over a period of years. Most of the work so far has concentrated on systems with compositions and configurations similar to the Demonstration reactor. Additional critical experiments will be needed for the larger LMFBR systems, and these are being planned at this time. A set of potential physics problems are emerging as a result of this planning. Also, benchmark critical experiments are currently in progress for the Gas Cooled Fast Reactor (GCFR) program. From the initial results it is apparent that the analytical techniques developed for the LMFBR are not completely adequate for the GCFR, a system that in many ways is very similar to the LMFBR. Serious discrepancies have been found in the calculated eigenvalue and in the prediction of the steam-entry experiment. Additional work is needed to validate techniques for handling anisotropic diffusion and for the calculation of hydrogen in a fast system.

The differences in composition and configuration between the LMFBR meltdown cores and their undamaged references are much greater in most ways than the differences among the various fast-reactor designs for which critical experiments have been performed. The only critical assembly measurements on simulated meltdown cores were made in ZPR-III Assemblies 27 and 28 and in the current CRBR-EMC program at ZPPR. As discussed in detail in the latest monthly report, none of these measurements provide an acceptable test of the Monte Carlo analytical techniques needed to calculate meltdown cores. There are a number of things wrong with the Assembly 27 and 28 measurements, one of the most important of which is the core compositions. These cores contain no plutonium, sodium or oxygen, certainly three of the key materials in an LMFBR. One of the important elements in the validation of the Monte Carlo analysis is to determine whether the ENDF/B cross sections are adequate for the range of compositions found in meltdown configurations. The CRBR-EMC measurements at ZPPR simulate only the initial stages of a severe meltdown accident. Only a small fraction of the core is distorted and the maximum reactivity change is still small (<$2). These measurements cannot be used to evaluate the adequacy of the Monte Carlo analysis for predicting meltdown configurations.

In summary then, the arguments for meltdown critical experiments are as follows: The LMFBR data and codes have been extensively tested, and in many cases adjusted, for cores similar to the DEMO. Experience shows that when even small design changes are made, analytical difficulties start to appear. The meltdown cores represent very significant changes from the standard undamaged DEMO design. There are no acceptable critical experiments by which to test and calibrate the codes and data used to calculate meltdown cores. Based on previous experience, difficulties in predicting the meltdown cores are to be expected. Critical experiments are therefore needed both to identify any possible analytical problems and to provide the reference integral data needed to validate improved codes and basic cross-section data. The critical experiments should be specifically designed to provide a test of analytical techniques, primarily Monte Carlo, used to calculate meltdown configurations. Without the critical experiments, the predictions of meltdown configuration will remain unvalidated and uncertain.

## B. Relationship of the Safety Related Critical Experiment to Other Critical Experiment Programs

The two other critical experiment programs that have produced data relevant to the evaluation of meltdown configuration are ZPR-3 Assemblies 27 and 28 and the current program at ZPPR, the Clinch River Breeder Reactor Engineering Mockup Core Program (CRBR-EMC). Data and evaluations from these programs are currently becoming available and will impact the current planning activity. The results of the VIM Monte Carlo analysis of ZPR-3 Assembly 27 and Assembly 28 are now available. Most of the data from the CRBR-EMC HCDA meltdown simulation experiments are now available; however, the detailed post-evaluation of these data is just beginning. Both of these programs have produced useful integral data but neither provides the needed validation of the meltdown analysis techniques (i.e., Monte Carlo). (Neither program was designed for this purpose.) The evaluation of these programs is part of this critical experiment planning activity. Their relationship to the current planning activity is discussed in more detail below.

### 1. ZPR-3 Assemblies 27 and 28

These experiments were done at ZPR-3 in the early 1960's and have been analyzed at ANL using the VIM Monte Carlo code. They represent two steps in a very severe meltdown of a small two-zone fast reactor. These comprise significant changes in core configurations and in this sense they represent a good test of the Monte Carlo analysis. There are a number of reasons why these experiments have only limited usefulness and why they do not constitute an adequate test of the Monte Carlo. These are listed below.

a. These assemblies were fueled with uranium metal and used aluminum to simulate the coolant. They contained no plutonium, sodium, or oxygen, three of the most important materials in an LMFBR. One of the key elements in the validation of the Monte Carlo analysis is to determine whether the ENDF/B cross sections are adequate for the range of compositions found in meltdown situations. These cross sections have been evaluated, and adjusted in subtle ways, for the nominal LMFBR compositions. The compositions in a meltdown configuration can be very different, and therefore emphasize different cross sections and ranges of energy. Therefore there is absolutely no assurance that the ENDF/B cross sections will behave well in these cases.

b. Only a single number from Assemblies 27 and 28 (i.e., the $k_{eff}$) is available for comparison with the Monte Carlo analysis, e.g., no reaction rate distributions were measured. Any agreement obtained could be due to cancelling errors or simply fortuitous.

c. Assemblies 27 and 28 had an extremely complicated loading and they were built nearly 15 years ago. Considerable effort was required to locate and interpret all the original loading diagrams and a number of inconsistencies were discovered. There is a considerable uncertainty as to the exact loading of these cores and this must be considered when interpreting the results of the Monte Carlo analysis.

d. Assemblies 27 and 28 simulated severe meltdown configurations. No undamaged version of these cores was constructed nor were there any intermediate configurations. An undamaged configuration is especially important

in order to normalize the analysis of the meltdown configurations. Both the meltdown configurations and the undamaged reference are needed to adequately validate the analysis. Intermediate configurations are also needed to help determine where things start to go wrong in cases where there are significant discrepancies between the analysis of the reference undamaged and the final severe meltdown configurations.

e. Because of the complicated drawer-loading arrangements, Assemblies 27 and 28 are very difficult to set up for $S_n$ or diffusion-theory calculations. After the validation of the Monte Carlo results by comparison with experiments the next step is the use of Monte Carlo to evaluate $S_n$ or diffusion-theory codes for these configurations. It would be helpful if the critical experiment configurations were chosen to be amenable to modeling in $S_n$ or diffusion theory.

The evaluation of Assemblies 27 and 28 is a useful step in the validation of the Monte Carlo for meltdown configurations. They are the only experiments currently available for this purpose. Based on the above comments it is apparent, however, that additional experiments are needed to complete the validation process.

2. CRBR-EMC (ZPPR-5)

The first phase of the CRBR-EMC program is currently in progress with a completion scheduled for December 1975. A large part of this program is a set of experiments designed to simulate the initial stages of a core-meltdown accident. A series of snapshot configurations were constructed in the mockup core and measurements were made of $\Delta k_{eff}$, of the reactivity traverses for all the important core materials, and of power distributions in the core. The snapshot configurations were derived from a SAS calculation of a loss-of-flow accident in the CRBR. The actual experimental configurations were somewhat simplified from the analysis predictions in order to facilitate both the analysis and the experimental loadings.

In the initial part of the experiment, sodium was voided from the core and upper axial blanket in four major steps with four substeps per major step. At the final step over one half of the core and over one half the upper axial blanket were voided.

In the next part of the experiment, about 30% of the steel from the 30 central subassemblies was slumped outward axially from the center of the core. This was done in two major steps with two substeps each. The two major steps represented steel slumping to regions ±9-in. from the axial midplane of the core and then ±14-in. from the axial midplane of the core.

The final step represented fuel slumping in the 18 central subassemblies. In these cases all the fuel in the slumped region was moved. Fuel from the regions ±(7 to 14) in. from the core midplane was slumped into the region of -7 to +7 in. Thus, the fuel density in the central region was doubled and no fuel was in regions from 7 to 14 in. In fact these regions were nearly voided since the sodium and part of the steel had previously been removed. This was called the "slump-in" configuration and represented maximum reactivity addition. The next part of the fuel slumping experiment, called the "slump-out" configuration was exactly the opposite. The fuel from the -7 to +7 in. region was moved to the two regions ±(7 to 14) in.

This whole set of experiments was done in a core simulating the end of the 1st cycle (i.e., control rods withdrawn). It is now being repeated (in reverse order) in a core representing the beginning of the initial cycle (i.e., control rods inserted).

The questions are then (1) what has been learned from these experiments and (2) how do they affect the planning for the additional meltdown experiments? The first question cannot be answered completely at this time since the post-analysis of these experiments has just barely started. Some preliminary results are available, however, based on the preanalysis which was part of the planning for these experiments.

a. The sodium void worth showed a very significant axial asymmetry. This was due to the parked rods in the upper axial blanket and the asymmetric way in which the sodium was voided. The results from the case with the control rods inserted, not yet available, may help separate these two effects. The preanalysis has done a fairly good job of predicting these experiments. More careful postanalysis indicates that some of the accurate predictions of the preanalysis were fortuitous.

b. In the case of the steel slumping, the preanalysis underpredicted the measured values by 20-30%.

c. The major discrepancy between the preanalysis and the experiments occurred for the fuel-slumping case. The "slump-in" positive worth was underpredicted by about 20% but the "slump-out" worth was over a factor of five less negative than predicted. This result was reported in the previous quarterly report, ANL-75-67. In the "slump-out" case there are two competing effects: (1) the reactivity loss due to movement of fuel away from the core center and (2) reactivity gain due to increased fuel density in a given region. The preanalysis, which was a k-difference calculation, simply did not handle these two effects properly.

It should be emphasized that these are preliminary conclusions based on the preanalysis and the preliminary evaluation of the data. The final results of the evaluation could change somewhat.

The second question was, how do these results affect the current planning program? To answer this question, the original objectives of the current planning effort were reviewed. These, very briefly, were (1) validation of the Monte Carlo analysis for meltdown configurations and (2) providing directly useful reactivity data on prototypical meltdown configurations. In the current planning effort it has become apparent that these are not compatible objectives if one interprets prototypical to mean similarity of composition, configuration and whatever else possible. The main problem is configurational similarity. The best core design to test and validate the Monte Carlo analysis is not a core that is configurationally prototypical of the CRBR. The desirable features of a core designed to test the Monte Carlo analysis are discussed in the next section. Alternately the experiments performed on the prototypical CRBR-EMC will provide no meaningful test of the Monte Carlo analysis. The meltdown zone was composed of only 18 subassemblies, a small fraction of the total core, and the maximum reactivity change was less than $2. The

Monte Carlo calculation could be grossly in error in the fuel-melt region and it would not significantly alter the overall core results. On the other hand the CRBR-EMC results are very prototypical of the initial stages of a loss-of-flow meltdown accident. This is the stage of the accident where prototypical results are meaningful. As the accident progresses further the course of events becomes much less certain, and prototypicality almost loses any meaning. It is felt that the current CRBR-EMC measurements provide a useful set of prototypical meltdown experiments for a Demo-sized core and the second objective of the current meltdown core planning activity is largely satisfied by the CRBR-EMC results. This allows the current planning to concentrate on meeting the primary objective, that of validating Monte Carlo analysis techniques for use in meltdown analysis. This is the course that the planning is now taking.

In summary then, the key conclusions resulting from the examination of the relationship of this critical experiments planning activity and previous critical experiments programs are as follows.

a. The Assembly-27 and -28 measurements cannot provide adequate validation of Monte Carlo for meltdown configuration analysis.

b. The CRBR-EMC measurements can largely satisfy the second objective of the safety-related critical experiments program; that of providing directly useful reactivity data on prototypical DEMO meltdown configuration. However,

c. the CRBR-EMC measurements do not provide a test of Monte Carlo analysis of a severe meltdown configuration. Therefore,

d. the proposed safety-related criticals should concentrate on meeting the first objective of the program, that of validating the Monte Carlo analysis techniques for use in the analysis of meltdown configuration.

## C. Summary of Core Design and Program Characteristics

A proposed reference of core designs and a preliminary program plan were included in the January-through-March 1975 Quarterly Report, ANL-75-31. Some modifications to this program have now been made, primarily as a result of the clarification of objectives discussed in the previous paragraph. The primary purpose of the meltdown-configuration critical experiments will be to validate the use of the Monte Carlo analysis for the general class of meltdown cores. The cores in the sequence of configurations will be specifically designed to test the Monte Carlo analysis, and no large effort will be made to make them configurationally prototypical of the DEMO. Typical LMFBR compositions will be used, however. The main characteristics of the core design and program are tabulated below.

### 1. Core Configuration

The reference core should have clean geometry to facilitate analysis and be small to emphasize leakage effects. The distorted cores should have relatively large voided regions and regions of high fuel density. The perturbed regions should represent significant fractions of the total core volume.

Regions of sodium, structural, blanket and absorber will be included at various stages in the sequence. The primary objective is to simulate each of the key features common to nearly all meltdown configurations.

2. Core Composition

The reference core will have a typical LMFBR composition with the approximately correct volume fractions of heavy metal, structural materials and sodium. Because of the smaller core size, the enrichment will be more typical of the DEMO outer-core composition than of the inner-core composition.

3. Core Geometry

In order to facilitate the setup and use of the standard $S_n$ and diffusion-theory calculations a relatively simple core geometry will be specified. The core designs should allow use of RZ models.

4. Unit-Cell Designs

The number of unit-cell designs is to be minimized in order to simplify the setup of the Monte Carlo analyses. The large number of different unit-cell designs in ZPR-3 Assembly 27 greatly complicated the Monte Carlo analysis of this system.

5. Number of Configurations in Sequence

The program should contain a number of configurations (approximately five) ranging from the reference (undamaged) configuration to the final meltdown configuration. This will allow an evaluation of where things start to go wrong in case there is a significant discrepancy between the analysis and the experiments for the final configuration. Consideration is also being given to including a $B_4C$ region in some of the meltdown configurations. Analysis has suggested that $B_4C$ is a more effective reflector than $UO_2$ in certain meltdown configurations. The experiments would check this effect.

6. Midplane Symmetry

Most realistic meltdown configurations will contain some axial asymmetry. The ZPR-3 Assembly-27 core had the fuel compacted at the bottom. It is relatively easy, however, to design an axially symmetric core that captures the essential features needed to validate the Monte Carlo analysis. In addition, an axially symmetric core allows much more rapid accumulation of statistics in the Monte Carlo analysis (symmetry can be used to limit the volume of the calculational model) and has operational advantages in that the safety analysis of the criticals is considerably simplified. With the symmetric core the same amount of fuel is loaded into each half of the assembly. Questions concerning the possible criticality of a single half are avoided. Some degree of axial asymmetry will certainly be possible, however, as long as the fuel loadings in each half of the critical assembly are approximately the same. It is probable that some of the configurations will contain some axial symmetry but not to the same degree as ZPR-3 Assembly 27.

7. Reference Meltdown Configuration

The reference final meltdown configuration was tentatively taken to be an axially symmetric loading with compacted fuel at the axial midplane. Regions of void, structural and blanket will be included in the axial directions. Loading sequences similar to those described in ANL-75-31 are still being considered.

8. Experimental Data

The measurements will include most of the standard ZPR measurements - criticality, reactivity worth, reaction rates, safety coefficients, spectra, etc. The list of experiments is similar to those described in Table VII of ANL-75-31. Once the effort is expended to actually construct the meltdown configurations it is felt that the small additional time required to do a rather complete set of measurements is certainly justified. The Monte Carlo analysis is capable of predicting the reaction rate in large (probably planar) foils. These can be simulated in the criticals by using a number of small irradiation foils loaded into the same plane.

D. Core-Design Calculations

The general characteristics of the core design outlined in the previous paragraph are providing the guidelines for the core-design calculations. A number of alternate unit-cell plate loading arrangements have been defined and analyzed. It is expected that the actual design will be chosen from among these loadings. Each of these loadings was chosen to give a relatively small, leaky core, and to have a typical LMFBR composition. The unit-cell designs are relatively simple and, with two exceptions, are symmetric.

The unit cells, denoted as Compositions 1, 2, 3, 4 and 5 are shown in Fig. 1. The compositions are characterized in Table I by $^{239}Pu$ atom density and fissile enrichment. The other materials tabulated for each composition are stainless steel (or iron in the case of the $Fe_2O_3$), sodium and oxygen. For purposes of comparison the $^{239}Pu$ atom densities for the CRBR inner and outer cores (beginning of initial cycle) are $1.080 \times 10^{21}$ and $1.575 \times 10^{21}$ atoms/cm$^3$, and the enrichments in the inner and outer cores are 0.1577 and 0.2291. The steel, sodium and oxygen concentrations are roughly matched to the LMFBR values.

Compositions 1, 2 and 4 turned out to be somewhat too reactive and, therefore, it is expected that the final design of the reference core will be similar to compositions 3 or 5. Composition 3 has the advantage that it is a simple, symmetric, one-drawer-unit-cell design while composition 5, the ZPPR-2 outer core composition, is a two-drawer unit cell. ZPPR-2 was the initial DEMO two-zone benchmark. It contained no simulated control rods and, consequently, its fissile atom densities and enrichments were somewhat lower than the CRBR values. Compositions 3 and 5 are intermediate to the CRBR inner and outer core values for both $^{239}Pu$ atom density and enrichment. These are, therefore, typical LMFBR compositions.

The analysis summarized in Table I was performed as follows. A series of homogeneous one-dimensional (spherical) multigroup diffusion calculations was performed for the unit-cell compositions. For each composition, homogeneous (27 broad-group) cross sections were obtained using the fundamental-mode

TABLE I. Safety Related Critical Assembly Planning, Reference Core Design Studies

| Composition | 1 | 2 | 3 | 3a | 3b | 3c | 4 | 5 |
|---|---|---|---|---|---|---|---|---|
| | | | | Bare Homogeneous Spherical Models | | | | |
| Critical Buckling | 0.0027882 | 0.0028591 | 0.0021743 | 0.0046347 | 0.0037870 | 0.0067263 | 0.0028787 | 0.0018417 |
| $k_\infty$ ($B^2 = 0.0$) | - | - | - | 1.68839 | 1.59388 | 1.71750 | - | 1.43601 |
| Critical Radius, cm | 59.50 | 58.75 | 67.37 | 46.15 | 51.05 | 38.31 | 58.55 | 73.21 |
| Volume, ℓ | 882.2 | 849.6 | 1281.0 | 411.6 | 557.3 | 235.4 | 840.9 | 1643.3 |
| Fissile Pu, kg | 632.0 | 608.7 | 763.9 | 392.9 | 490.0 | 280.0 | 602.4 | 882.9 |
| $^{239}$Pu Density × $10^{21}$ | 1.779 | 1.779 | 1.486 | 2.376 | 2.082 | 2.972 | 1.779 | 1.335 |
| Enrichment, $\frac{\text{Fissile}}{\text{Heavy Metal}}$ | 0.1651 | 0.2007 | 0.2214 | 0.2334 | 0.2092 | 0.2214 | 0.2564 | 0.1872 |
| | | | | Reflected Homogeneous Spherical Models (40 cm Blanket) | | | | |
| Reflector Savings, cm | - | 14.33 | 15.59 | 11.52 | 12.06 | 9.42 | - | 15.69 |
| Core Radius, cm | - | 44.42 | 51.78 | 34.63 | 38.99 | 28.89 | - | 57.52 |
| Core Volume, ℓ | - | 367.0 | 581.4 | 173.9 | 248.3 | 101.0 | - | 797.2 |
| Fissile Pu, kg | - | 263.0 | 346.7 | 166.0 | 207.2 | 120.4 | - | 428.3 |

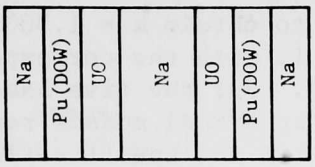


UNIT CELL 1

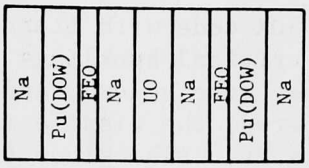


UNIT CELL 2

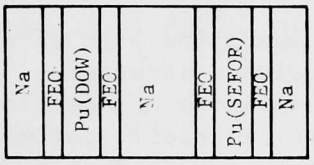


UNIT CELL 3

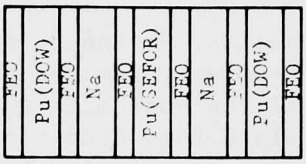


UNIT CELL 3A

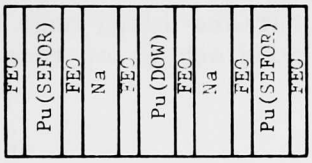


UNIT CELL 3B

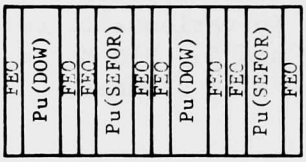


UNIT CELL 3C

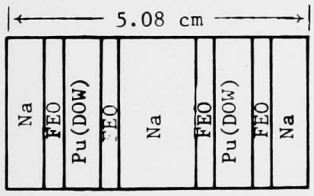


UNIT CELL 4

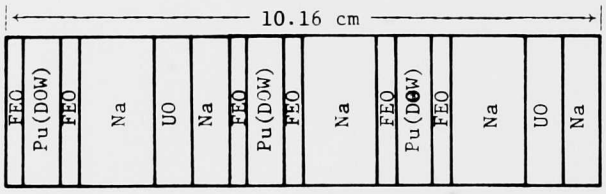


UNIT CELL 5 (TWO DRAWERS)

KEY:

UO = $U_3O_8$ Plate

Na = Na Can

FEO = $Fe_2O_3$ Plate

Pu (DOW) = Pu/U/Mo CAN (.282/.691/.025, $^{239}Pu/Pu = 0.907$)

Pu(SEFOR) = Pu/U/Mo CAN (.195/.779/.026, $^{239}Pu/Pu = 0.870$)

Fig. 1. Unit Cell Plate Loadings

option of the SDX code with iteration upon buckling to obtain k = 1.0000. Values of the critical bucklings are given in Table I, with the corresponding critical radius, core volume, and fissile-Pu loading. For the five base compositions considered, the fissile masses for the bare spherical models ranged from 600-900 kg Pu. Also given in Table I are the critical specifications for reflected spherical models. These were obtained by adding a 40-cm-thick blanket (correponding to ZPPR-2 inner core axial blanket composition) and adjusting the core radius to achieve criticality. The reflector savings was approximately 15 cm and reduced the fissile loadings to approximately 260-430 kg Pu.

Compositions 3a, 3b and 3c are variations of composition 3 in which the sodium is progressively removed and replaced with fuel and structure. In composition 3c, all the sodium is removed. These are candidate compositions to be used to simulate fuel densification regions. Critical radii, volumes and fissile masses are also listed for these cases for both the reflected and bare homogeneous models. It can be seen that these compositions (especially 3c) are very reactive.

Two-dimensional cylindrical calculations for both the clean reference core and cores in various stages of a meltdown accident are being made for compositions 3 and 5. VIM Monte Carlo analyses for some subset of these configurations are also planned.

# REFERENCES

1. H. Hummel, Kalimullah, P. Pizzica, "Pump Coastdown Calculations for a Model of a 4000 MWe Oxide-Fueled LMFBR," in Physics of Reactor Safety Quarterly Report, January-March 1975, ANL-75-31, p. 7.

2. P. B. Bleiweis, D. Okrent and W. E. Kastenberg, "A Comparison Study and Analysis of Models for 4000 MWe LMFBR Hypothetical Accidents," Proceedings of the Fast Reactor Safety Meeting, Beverly Hills, California, April 2-4, 1974, CONF-740401-P3, pp. 1322-1332.

3. P. Bleiweis, B. Ganapol, C. Bowers, P. Abramson and D. Weber, "A Comparison of Three Disassembly Models for a 1000 MWe Fast Breeder Reactor," Trans. Am. Nucl. Soc., 22, November 1975.

4. J. F. Jackson and R. B. Nicholson, "VENUS-II, an LMFBR Disassembly Program," ANL-7951, September 1972.

5. T. McLaughlin, private communication.